

# An Experimental Comparison of Thermal Performance: Smooth and Inner-Grooved Closed Loop Pulsating Heat Pipes in Different Angles

Rostam Akbari Kangarluei<sup>a</sup>, Majid Abbasalizadeh Ranjbari<sup>b\*</sup>, Ahad Ramezanzpour<sup>c</sup>

<sup>a</sup> Department of Mechanical Engineering, Urmia University, Urmia, Iran, Email: [ro.akbari@urmia.ac.ir](mailto:ro.akbari@urmia.ac.ir)

<sup>a</sup> Department of Mechanical Engineering, faculty of Tabriz, Technical and vocational University (TVU), Tabriz, Iran, Email: [rsakbari@tvu.ac.ir](mailto:rsakbari@tvu.ac.ir)

<sup>b\*</sup> Corresponding Author, Department of Mechanical Engineering, Urmia University, Urmia, Iran, Email: [m.abbasalizadeh@urmia.ac.ir](mailto:m.abbasalizadeh@urmia.ac.ir)

<sup>c</sup> School of Engineering and the Built Environment, Anglia Ruskin University (ARU), Bishop Hall Lane, Chelmsford, Essex, UK, Email: [ahad.ramezanzpour@aru.ac.uk](mailto:ahad.ramezanzpour@aru.ac.uk)

## Abstract

Pulsating Heat Pipes are ideal for compact cooling applications such as electronic cooling. In this experimental research, the thermal performance of Inner-Grooved Pulsating Heat Pipes (IGPHP) and Smooth Pulsating Heat Pipes (SPHP) compared using distilled water in different angles. The inclination angles of 0°, 5°, 15°, 30°, 50°, 70°, and 90°, and the input heat range of 50-300W were studied. The results show that the optimum filling ratio is 60% for IGPHP and SPHP. The study shows that in constant Input heat, the thermal resistance of IGPHP is lower than SPHP and the effective thermal conductivity of IGPHP is higher compared to SPHP. The average reduction of the thermal resistance of IGPHP compared to SPHP was found 21% across all angles and input heat powers; however, the average reduction was 49% for the angle of 5° across all input heat powers. The dryout phenomenon for IGPHP took place at 0° and the input heat of 100W, while for SPHP, this occurred at 5° and 250W. The overall comparison shows that IGPHP is an even better alternative to SPHP in higher capacity applications.

**Keywords:** Pulsating heat pipe, Inner-groove, Inclination angle, Filling ratio, Thermal resistance

## Nomenclature

Cross-sectional area (m <sup>2</sup> )	A
Specific heat capacity at constant pressure	C <sub>p</sub>
Diameter (m)	D
Hydraulic diameter (m)	D <sub>h</sub>
Height of fin (mm)	H <sub>f</sub>
Electric Current (Amp)	I
Thermal conductivity coefficient (W/mK)	K
Length (m)	L
Mass flow rate (kg/s)	$\dot{m}$
Number of Grooves	N
Outer Diameter (mm)	OD
Input heat power (W)	Q
Thermal Resistance (k/W)	R

## Greek Symbol

Apex angle (degree)	$\alpha$
Helical angle (degree)	$\beta$
Surface tension (N/m)	$\sigma$
Density (kg/m <sup>3</sup> )	$\rho$
Heat loss coefficient	$\phi$

## Subscript

Condenser	c
Evaporator	e
Thermal	t
Voltage	v
Current	i

Temperature (C)	T	Vapor	vap
Thickness of Wall (mm)	TW	Effective	eff
Uncertainty	u	Inlet	in
Voltage (volt)	V	Outlet	out
		Liquid	liq
		Critical	crit
		Repetition	rep

## *Abbreviations*

PHP	Pulsating Heat Pump
SPHP	Smooth Pulsating Heat Pump
IGPHP	Inner-Grooved Pulsating Heat Pump
FR	Filling Ratio

## 1. Introduction

The demand for higher power, efficiency, and downsizing in industry, including electronic equipment, requires technologies with high heat flux capabilities. Heat pipes, while being low cost and without any moving parts, can transfer large amounts of heat in a small temperature difference. In 1990, Pulsating Heat Pipes (PHPs) were first introduced by Acachi [1]. PHPs are a type of two-phase heat transfer devices that transfer heat between the evaporator and the condenser through pulsating and continuous motion. PHPs are particularly advantageous over the conventional heat pipes due to the simultaneous latent and sensible heat transfer [2].

Many parameters affect the performance of PHPs, including the properties of the working fluid, filling ratio, and inclination angle as well as internal diameter, the number of revolutions, cross-sectional structure, and internal structure of the pipe. The effects of these parameters have been investigated in the literature; These include increasing the inner diameter (within the critical diameter range) or decreasing the length of the evaporator zone to improve start-up pulsation [3], increasing the pipe diameter, despite the reduction in pulsation frequency, to increase the heat transfer flux [4], increasing of vaporization latent heat to reduce thermal resistance [5], and increasing the number of PHP cycles to reduce thermal resistance and increase effective thermal conductivity [6]. Several researchers have investigated the advantages of PHPs including the high performance of PHPs at low temperature difference energy recovery systems in air conditioning [7] and lower thermal resistance of PHPs compared to a solid copper plate in low temperature difference electronic cooling system [8].

The experimental study by Borkar and Pachghare [9] shows that the thermal performance of Smooth Pulsating Heat Pipe (SPHP) is dependent on the flow pattern and is optimum in a continuous unidirectional cyclic flow. Water is widely used as working fluid in PHPs, however, at low temperatures, other fluids such as R134a, ethanol and acetone are used depending on the operating temperature range. Most experimental studies show that the optimal filling ratio, depending on the working fluid, in PHPs is in the range of 40 to 70% [10-12].

Several studies show that low inclination angle of PHPs, due to gravity, increases the thermal resistance; the optimum angle, depending on the filling ratio and the input power, is between 60° to

90° [13-16]. Furthermore, in higher number of piping turns, the dependency between thermal performance and the inclination angle is weaker [17].

The effects of pipe surface structure on the performance of PHPs have been studied in the literature. Betancur et al. [18] created a rough surface by sanding a smooth copper surface by standard sandpaper with Grit N1200 and used in a PHP. The results showed that the surface roughness increases the number of vapour nucleation sites; therefore, facilitating the change of phase in the evaporator and the pulsation start-up at lower filling ratios. The literature shows that the heat transfer rate of Inner-Grooved Pulsating Heat Pipes (IGPHP) is higher due to the increase in the heat exchange surface compared to smooth surface structure [19, 20]. Studies by Hao et al. [21, 22] show that the hydrophobic condenser and hydrophilic evaporator surface structures increase the pulsation amplitude and the working fluid velocity; therefore, increasing the heat transfer rate. Ji et al. [23] increased hydrophilicity on the pipe surface by using a copper oxide microstructure coated on the inner pipe wall. The results showed that hydrophilicity significantly increases the thermal performance of PHPs.

The sintering of pipe surface has shown improvement on heat transfer in PHPs, however, this is a more complex process and less effective in smaller pipe diameters [24]. In IGPHPs, the micro-axial grooves due to capillary effects, act as a miniature pump, facilitate the return of working fluid from condenser to the evaporator, therefore increasing both sensible and latent heat transfers [25-27].

Zhang et al. [28] experimentally investigated the effect of cupric oxide coating, hydrophilic nanostructured, and concluded that the condenser of PHP had the highest heat transfer enhancement. Qu et al. [29] experimentally compared the thermal performance of closed SPHP and the IGPHPs with helical micro-grooves. The study utilised a device comprising three rounds of copper pipe with deionized water as the working fluid. The filling ratio in the study was 50%. The results showed that the use of micro-inner-grooved pipes was effective in the increase of thermal conductivity, reduction of the overall thermal resistance, and consequently improved thermal performance of the PHPs.

This experimental investigation aims to compare the thermal performance of closed IGPHPs and SPHPs in different orientation angles and input powers. The initial objective of this research is to evaluate the thermal performance for IGPHP and SPHP and obtain the optimum filling ratio in an inclination angle of 90°. Then, the study compares the thermal performance of IGPHP and SPHP in different inclination angles and input heat powers at the optimum filling ratio.

## 2. Experimental Setup

For the SPHP experiments, copper pipe with external and internal diameters of 4.76 mm and 3.86 mm, respectively, is used. The cross-section of the inner-grooved pipe for the IGPHP experiment has been shown in Fig. 1. The specification of the pipe and inner-grooves provided in Table 1.

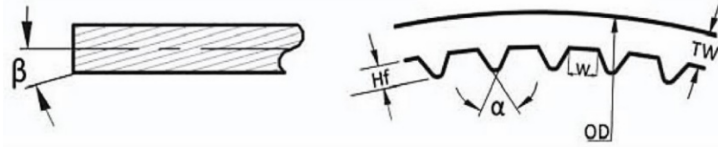
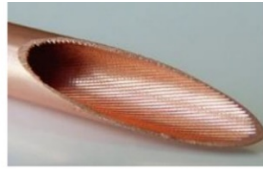


Fig. 1. Cross-Section of Inner-Grooved copper pipe (left: longitudinal apex angle, right: vertical cross section)

Table 1. Inner-Grooved copper pipe specifications (according to Fig. 1)

Outer Diameter (mm) OD	Thickness of Wall (mm) TW	Height of fin (mm) Hf	Apex angle $\alpha$ (degree)	Helical angle $\beta$ (degree)	Number of Grooves N
4.76	0.28	0.2	53	18	30

The setup of the experimental test rig at an angle of  $0^\circ$  and  $90^\circ$  shown in Fig. 2.



Fig. 2. The position of temperature sensors and system schematic

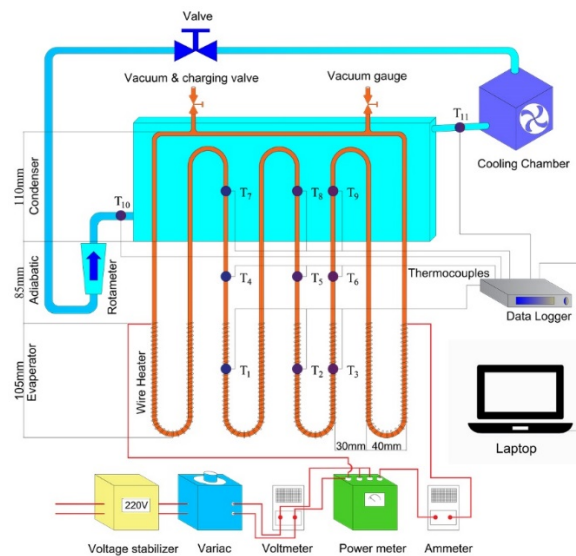


Fig. 3. Schematic of experimental setup and position of the sensors and the components

PHPs consist of three main parts: evaporator, adiabatic, and condenser. For both SPHP and IGPHP setup, the length of each part is 105 mm, 85 mm, and 110 mm, respectively (Fig. 3). A schematic of

the experiment, dimensions, position of the temperature sensors, and the system components have been shown in Fig. 3. Distilled water is used as the working fluid, and the copper pipe with four turns (U-shaped with a 30 mm gap between pipes) is used (see Fig. 3). The heat is applied by chrome-nickel-coated heating elements covered the copper tube in the evaporator. The input heat is adjusted using the Dereix SA Paris R212 variac and GANZ HE Wa2 wattmeter with an accuracy of 0.5W. Furthermore, the current and voltage measured using ammeter and voltmeter. The platinum JUMO PT100 temperature sensors were used to log temperature values with a data logger (Lutron BTM 4208SD) of 0.1 °C accuracy every 0.5 seconds. The water flow rate in the condenser was measured using a LUNA-A rotameter in the range of 0.03-0.35 GPM and an accuracy of 4%. The VE115N vacuum pump, capable of creating a vacuum pressure of up to 10 kPa, is used to pump the air from the heat. A vacuum gauge with an accuracy of 2 kPa was used to measure and control the vacuum and to ensure there are no leaks in the system.

The air is evacuated from the system by the vacuum pump, and then the system is filled with the working fluid (distilled water) to a specific filling ratio. To prevent heat loss in the evaporator and adiabatic area and to avoid the influence of the condenser by the ambient air, the whole system is fully insulated, and water is used as the cooling fluid in the condenser. In this study, experiments were performed with a filling ratio of 40%, 50%, 60%, and 70% and with an input heat of 50W, 100W, 150W, 200W, and 300W. The data were analyzed to select the best percentage filling ratio based on thermal performance. After determining the best filling ratio, the experiments were performed with the aforementioned input heat values and at orientation angles of 0°, 5°, 15°, 30°, 50°, 70°, and 90°.

In the inner-grooved pipes, hydraulic diameter  $D_h$  is used instead of internal diameter and is determined from the following equation [30].

$$D_h = \frac{4A \cos \beta}{NS} \quad (1)$$

In equation 1,  $\beta$  and  $N$  are the helical angle and number of microgrooves, respectively,  $A$  is the fluid flow cross-section in the pipe, and  $S$  is the wetted perimeter of one micro-groove.

Using the specifications of the inner-grooved pipe from Table 1, the hydraulic diameter of the pipe obtained as 2.65 mm.

A PHP must be designed so that the working fluid is pumped automatically. Considering the critical value of the Eötvös number  $\approx 4$ , the critical diameter obtained from equation 2 [31].

$$Eö = \frac{D_{crit}^2 g (\rho_{liq} - \rho_{vap})}{\sigma} \approx 4 \quad (2)$$

where  $D_{crit}$  is the maximum internal diameter,  $\sigma$  is the surface tension,  $\rho_{liq}$  and  $\rho_{vap}$  are the liquid and vapor phase density of the operating fluid, respectively, and  $g$  is the gravitational acceleration. In this study, distilled water has been used as the working fluid, so considering the properties of the distilled water, the critical diameter is about 5 mm, which is more than the inner diameter of the tube used in this study. In PHPs, the thermal resistance is used to compare and analyze the thermal resistance of the device; this is obtained from equation 3:

$$R_t = \frac{T_e - T_c}{Q} \quad (3)$$

In equation 3,  $T_e$  and  $T_c$  are the evaporator and the condenser average external wall temperatures, respectively and the thermal power supply to the evaporator of the PHP system shown by  $Q$ . The value of  $Q$  is obtained from equation 4:

$$Q = (1 - \varphi)V.I \quad (4)$$

where  $V$  is the input voltage,  $I$  is current, and  $\varphi$  is the heat loss coefficient.

The inlet heat transferred to the evaporator is then transferred to the condenser by working fluid (distilled water). The amount of heat transfer between the inlet and outlet of the condenser is obtained from equation 5 below:

$$Q_{out} = \dot{m} \cdot C_p(T_{out} - T_{in}) \quad (5)$$

In equation 5,  $\dot{m}$  is the mass flow rate of the water entering the condenser,  $C_p$  is the heat capacity of the water at constant pressure, and  $T_{out}$  and  $T_{in}$  are the temperatures of the water leaving and entering the condenser respectively. Along with the thermal resistance (equations 3), the effective thermal conductivity used as a criterion for the thermal performance of a PHP system, which is determined by equation 6 [32]:

$$K_{eff} = \frac{Q}{A} \frac{L_{eff}}{T_e - T_c} = \frac{1}{R_t} \frac{L_{eff}}{A} \quad (6)$$

where  $A$  is the cross-sectional area of the pipe based on the outside diameter and  $L_{eff}$ , the effective length between the evaporator and the condenser, obtained from equation 7 [33]:

$$L_{eff} = \frac{1}{2} (L_e + L_c) + L_a \quad (7)$$

In equation 7,  $L_c$ ,  $L_a$ , and  $L_e$  are the lengths of the condenser, evaporator, and adiabatic part, respectively.

The total uncertainty of each variable is calculated from equation 8, which is the root sum of squares of uncertainty related to repetition and the tools.

$$u_{total} = \sqrt{u_{tools}^2 + u_{rep}^2} \quad (8)$$

In equation 8,  $u_{tools}$  and  $u_{rep}$  are tools and repetition uncertainty respectively, and are calculated by dividing standard deviation to square root of number of measurements. The standard combined uncertainty has been used to calculate the input heat, thermal resistance, and effective thermal conductivity uncertainties. Calculations are carried out at a filling ratio of 60%, inclination angles of 30° - 90°, and across all the input powers (Table 2). According to equations 3, 4, and 6, the standard uncertainty for the heat input, thermal resistance, and effective thermal conductivity can be calculated from equations 9, 10, and 11 [34].

$$U_Q = \sqrt{\left(\frac{\partial Q}{\partial V} u_V\right)^2 + \left(\frac{\partial Q}{\partial I} u_I\right)^2} \quad (9)$$

$$U_R = \sqrt{\left(\frac{\partial R}{\partial T_e} u_{T_e}\right)^2 + \left(\frac{\partial R}{\partial T_c} u_{T_c}\right)^2 + \left(\frac{\partial R}{\partial Q} u_Q\right)^2} \quad (10)$$

$$U_{K_{eff}} = \sqrt{\left(\frac{\partial K_{eff}}{\partial L_{eff}} u_{L_{eff}}\right)^2 + \left(\frac{\partial K_{eff}}{\partial A} u_A\right)^2 + \left(\frac{\partial K_{eff}}{\partial R} u_R\right)^2} \quad (11)$$

where  $u$  for all variables has been calculated from equation 8. The average percentage of uncertainty for any variable  $T_e$ ,  $T_c$ ,  $Q$ ,  $R$ , and  $K_{eff}$  is calculated by the ratio of mean uncertainty divided by the mean of the variable. The mean values are calculated across the input heat powers (Table 2).

Showing the coverage factor by  $K_u$  and  $U$  as the uncertainty width, for  $K_u = 2$ , the maximum amount of uncertainty width can be calculated from equation 12.

$$U_{max} = U_{mean} \cdot k_u \quad (12)$$

Table 2 provides detailed calculations of uncertainty for condenser and evaporator temperatures, input heat power, thermal resistance, and effective thermal conductivity.

Table 2. Uncertainty percentage of main variables across range of the input heat powers

Input Heat Power, (w)	T <sub>c,ave.</sub> (°C)	U <sub>total,Tc</sub> Eq. 8	T <sub>e,ave.</sub> (°C)	U <sub>total,Te</sub> Eq. 8	Q (w)	U <sub>Q</sub> Eq. 9	R (k/w)	U <sub>R</sub> Eq. 10	K <sub>eff</sub> (w/m.k)	U <sub>Keff</sub> Eq. 11
50	29.0417	0.1947	64.7708	1.2611	50	0.2376	0.9075	0.0257	1496.53	42.297
100	33.3750	0.7764	69.6771	1.1193	100	0.3347	0.4352	0.0137	3149.17	97.696
150	37.0625	0.3168	76.3542	0.8973	150	0.4129	0.3044	0.0064	4466.47	93.211
200	40.7917	0.7175	81.6149	0.6458	200	0.4752	0.2323	0.0049	5841.53	121.631
250	44.1042	0.6899	88.2604	0.6714	250	0.5332	0.2029	0.0039	6672.21	127.194
300	47.0625	0.9569	93.9583	0.7552	300	0.5882	0.1802	0.0041	7512.20	169.753
Mean Values	38.5729	0.6087	79.1059	0.8922	175	0.4303	0.3771	0.0098	4856.35	108.630
Mean Uncertainty, %		1.5780		1.1272		0.2459		2.5900		2.2369
Max, %, Eq. 12		3.1560		2.2544		0.4918		5.1780		4.4738

### 3. Results and Discussion

#### 3.1. Optimum filling ratio

To select the best filling ratio, we performed the experiments in the vertical position for 40%, 50%, 60%, and 70% filling ratios. The results have shown in Fig. 4 for SPHP and IGPHP systems.

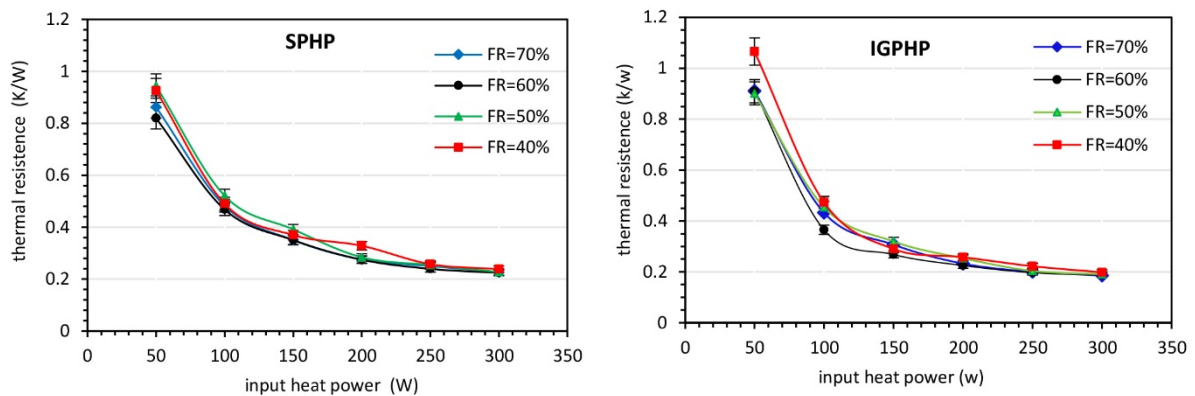


Fig. 4. Thermal resistance vs input heating power for various filling ratios, vertical SPHP left, vertical IGPHP right

The results of Fig. 4 show that the thermal resistance reduces as the input heating power increases. However, the slope of the reduction for the heating power input range of 50-150W is steeper compared to the range of 150W-300W. In both SPHP and IGPHP, better performance is expected as the input heating power increases, and thermal resistance reduces; however, the filling ratio of 60% shows lower thermal resistance compared to other filling ratios and therefore has better thermal performance is expected.

The results show that in very small values of input heating power, there is no pulsating motion taking place in the PHP due to insufficient force. Therefore, a minimum input heat power is required for the creation of pulsation. When the input heat exceeds the minimum requirement for pulsation, due to the transfer of liquid slug to evaporator and steam plugs to the condenser, the heat transfer rate increases, and the thermal resistance decreases. In this condition, there are a series of reciprocating pulsations occur inside the PHP, and the full circulation of the fluid flow does not occur, resulting in the weak performance of PHPs. As the inlet heat power increases further, the pulsation motions become relatively stable, and the operation of the PHP changes to a steady-state. An additional increase of inlet heat power results in a wider amplitude of the pulsations in the PHP to the extent that the fluid, in addition to reciprocating pulsation, tends to move forward, resulting in full completion of the fluid flow cycle in the PHP.

### 3.2. Thermal performance of SPHP and IGPHP in various inclination angles

A range of experiments conducted to compare the thermal resistance for SPHP and IGPHP, with the inclination angles of  $0^\circ$ ,  $5^\circ$ ,  $15^\circ$ ,  $30^\circ$ ,  $50^\circ$ ,  $70^\circ$ , and  $90^\circ$  and the input heating powers of 50W, 100W, 150W, 200W, 250W, and 300W.

For the SPHP in Fig. 5 (left), the high thermal resistance occurs for the inclination angles less than  $15^\circ$ . The dryout occurs at input heat of 50W for the angle of  $0^\circ$  and 250W for the angle of  $5^\circ$ .

For the IGPHP system, shown in Fig. 5 (right), at the angle of  $0^\circ$ , the thermal resistance is high, and the dryout phenomenon begins at 100W. It was observed that by changing the angle from  $5^\circ$  to  $0^\circ$ , the pulsation of the working fluid gradually decreases, and as a result, the value of evaporator temperature increases and the working fluid in the condenser section becomes almost static. In other words, due to lack of gravitational force in  $0^\circ$ , the fluid does not return to the evaporator from condenser, and dryout occurs in input heat of 150W.

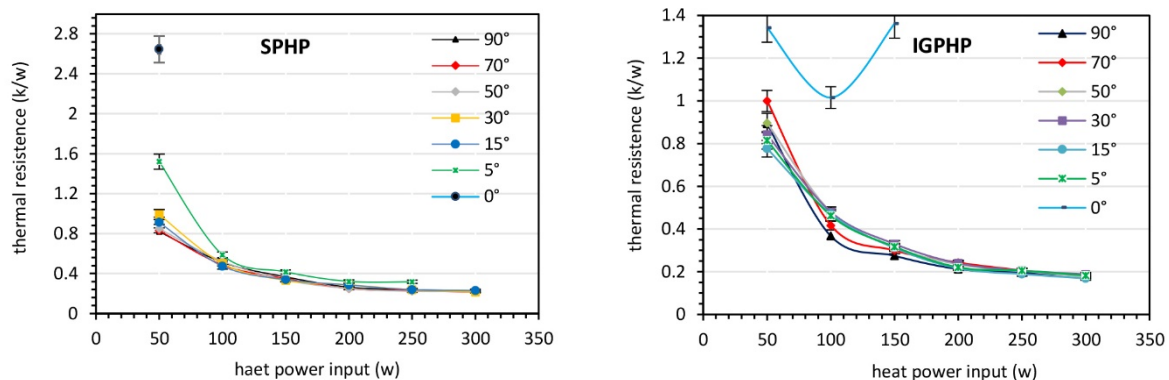


Fig. 5. Thermal resistance vs input heating power for various inclination angles, SPHP left, IGPHP right

In the IGPHP system, at low input heat values (50W), the value of thermal resistance at angles of  $70^\circ$  and  $90^\circ$  is greater than values at angles of  $5^\circ$ ,  $15^\circ$ ,  $30^\circ$ . This is likely due to the effect of the higher friction force as a result of the roughness of the inner grooves at angles of  $70^\circ$  and  $90^\circ$  compared to lower angles. Therefore, in comparison, the IGPHP start-up pulsation occurs later at angles of  $70^\circ$  and  $90^\circ$  in comparison to the SPHP system shown in Fig. 5 (left), which can be due to the smoothness of the inner surface of the pipe.

Due to inverse proportionality of the effective thermal conductivity and the thermal resistance, Fig. 6 (SPHP left, IGPHP right) show that the effective thermal conductivity increases with the increase of input heat. An important observation from Fig. 6 is that from an input heat of 250W to 300W, the

slope of increase of effective thermal conductivity is high in IGPHP in comparison to the SPHP. In comparison, while the effective thermal conductivity of the IGPHP, in general, is higher than SPHP, its performance could be even better in higher input heat capacities that would require further investigation for powers above 300W.

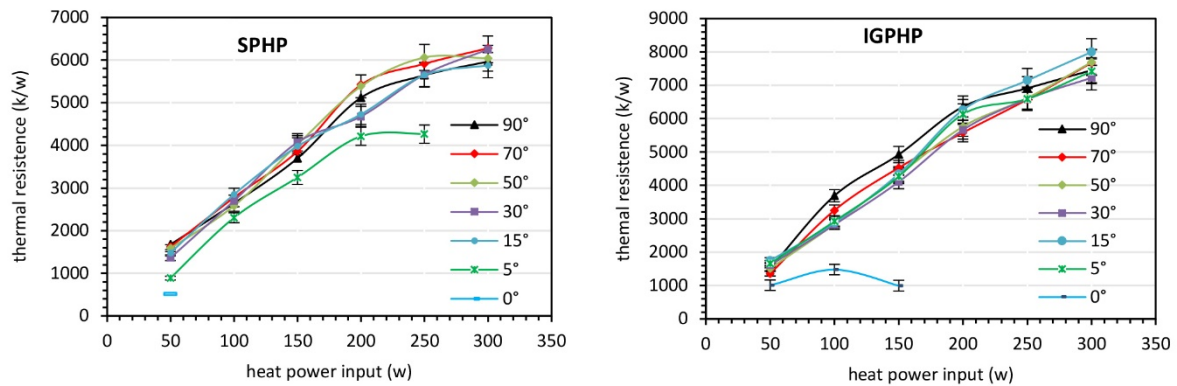


Fig. 6. Effective heat conductivity vs input heating power for various inclination angles, SPHP left and IGPHP right

In Fig. 7, and Fig. 8, the overall performance of the IGPHP and SPHP in various input heat powers and specific angles have been investigated. To be able to establish an accurate relationship between the variables, Fig. 7 shows the temperature variations in the condenser and evaporator for each angle and Fig. 8 shows the corresponding thermal resistance and effective thermal conductivity.

According to Fig. 7, at the angle of 90°, the temperature of the condenser in IGPHP and SPHP is almost the same in different capacities, but the evaporator temperature in SPHP is higher than the IGPHP for all input powers. This is due to the increased heat transfer surface area, swirling flow of the working fluid in the pipe, and improved capillary effect due to inner-grooved pipe helping the return of the fluid from the condenser to the evaporator. As input heat power increases, the amount of temperature difference between condenser and evaporator in SPHP increases more than IGPHP. Therefore, as shown in Fig. 8 (90°), the effective thermal conductivity is higher and thermal resistance is lower in IGPHP compared to the SPHP.

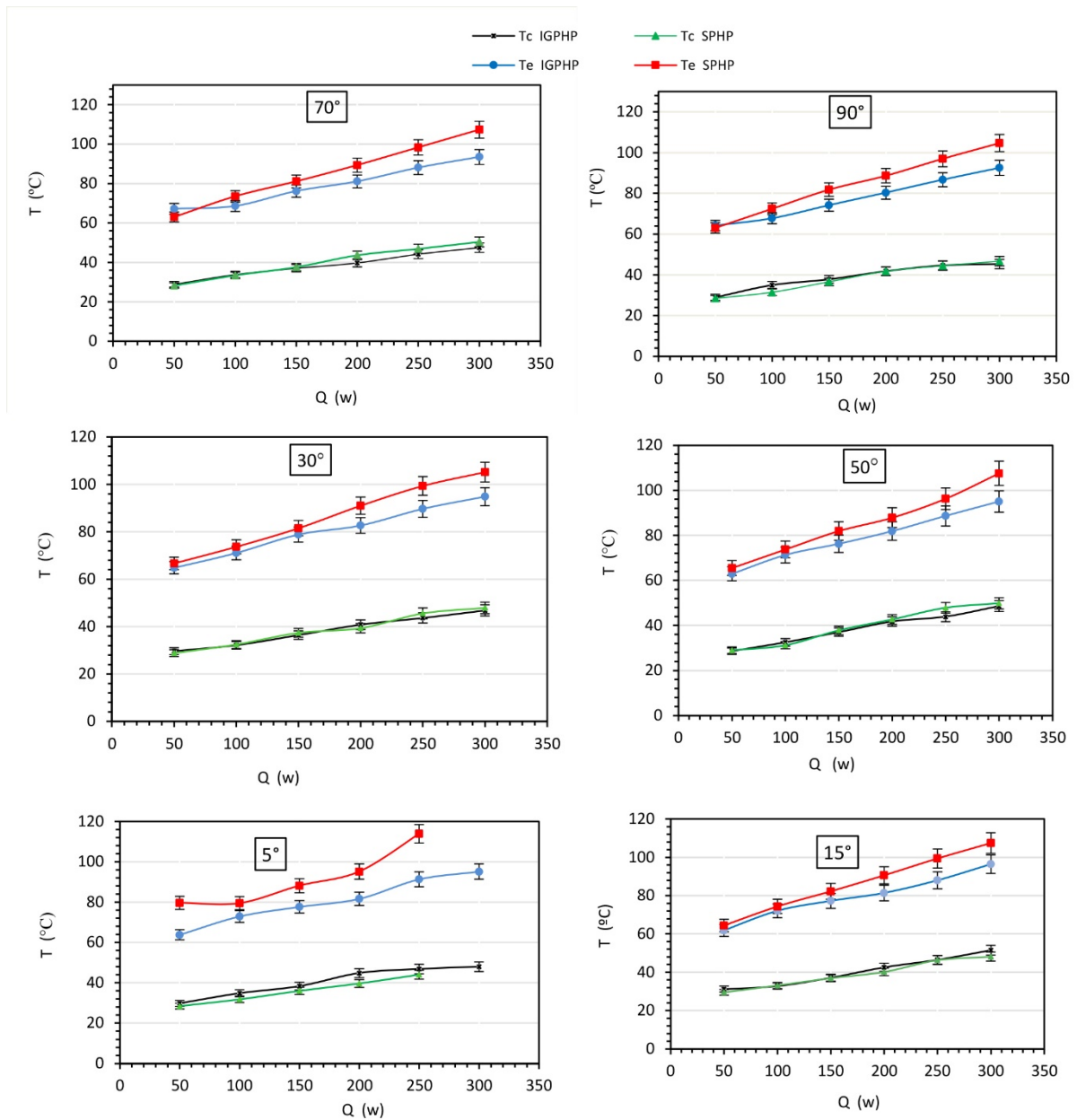


Fig.7. Evaporator and condenser temperature change for IGPHP and SPHP systems, various angles

The comparison of the results in other angles, in Fig. 7, and Fig. 8 shows similar behavior as for  $90^{\circ}$ . However, by reducing the inclination angle and approaching the horizontal setup, due to the reduction of the gravitational force, the movement of working fluid from the evaporator to the condenser is improved, and the capillary effect due to the inner grooves helps the return of the working fluid to the evaporator, so at angles close to the horizon ( $5$  and  $15^{\circ}$  angles) the IGPHP performs even better than SPHP.

Transient evaporator and condenser temperature values at  $15^{\circ}$  and  $90^{\circ}$  inclination angles for IGPHP and SPHP are compared in Fig. 12 and Fig. 13. The results show that in all inclination angles, the pulsation start-up in SPHP occurs earlier than in IGPHP, which could be due to the high friction in IGPHP, as a result of inner grooves. However, due to low gravitational force in smaller inclination angles, the start-up pulsation in IGPHP occurs close to the SPHP (Fig. 12). Therefore, IGPHP system performs better at low angles close to the horizon.

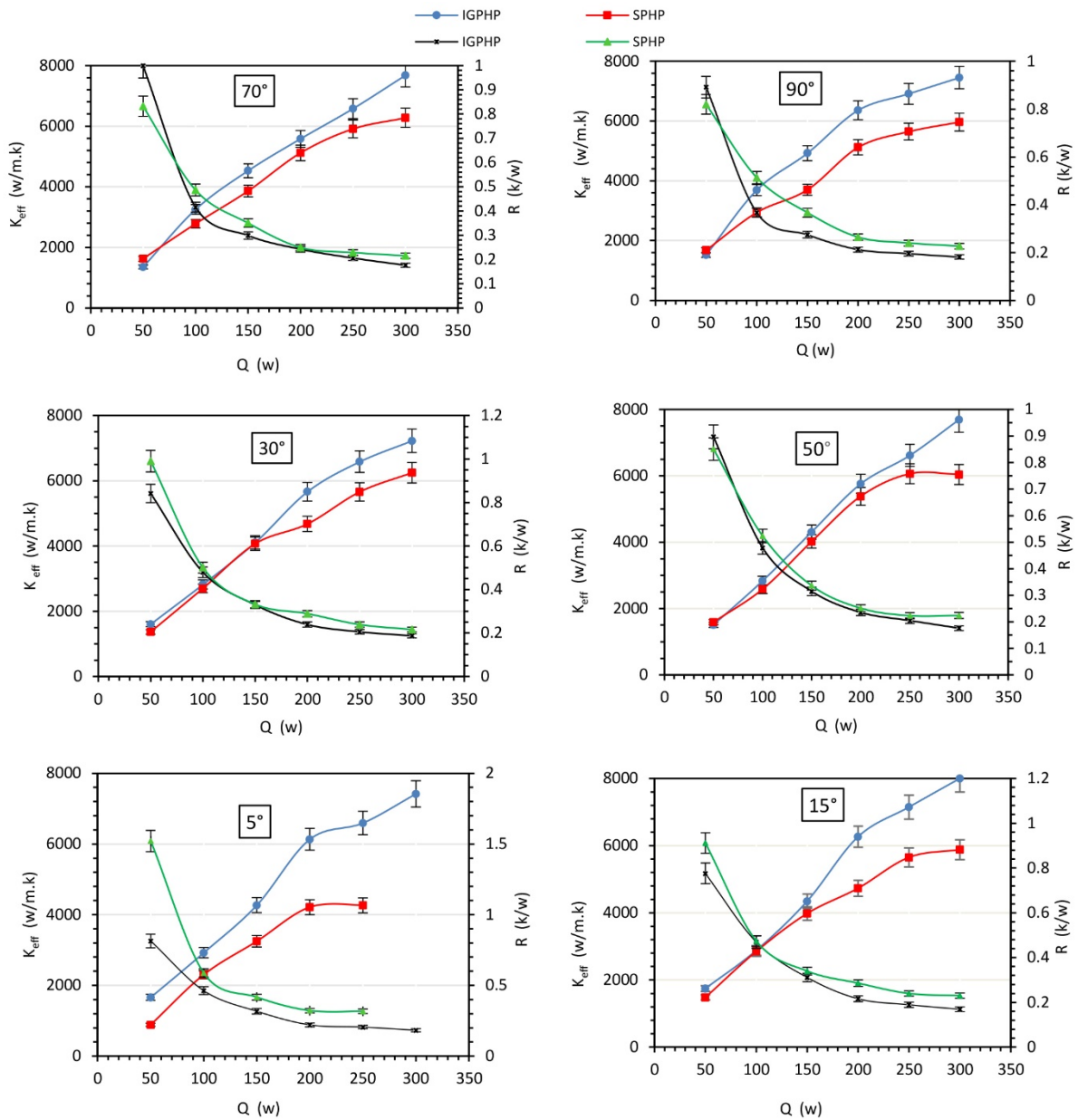


Fig.8. Effective thermal conductivity and thermal resistance for IGPHP and SPHP systems, various angles

As shown in Fig. 9, each input heat value experimented for 10 minutes, and approximately after about 3 to 4 minutes, the average temperatures remain relatively stable by time. Due to the presence of inner grooves in IGPHP and increased friction between the working fluid and the pipe, in input heat power of 50W, the number of pulsations in IGPHP is less than SPHP. However, the amplitude of pulsations is higher. As the input heat power increases, the number of pulsations in IGPHP increases, and a layer of fluid covers the grooves; therefore, both the friction and amplitude of pulsations reduce.

It can also be observed that across the thermal capacities, the temperature difference between SPHP and IGPHP in the condenser, at two angles of 15° and 90° are small (see Fig. 9). However, the evaporator temperature difference between SPHP and IGPHP increases after 50W, which is consistent with the discussion for Fig. 7 and Fig. 8.

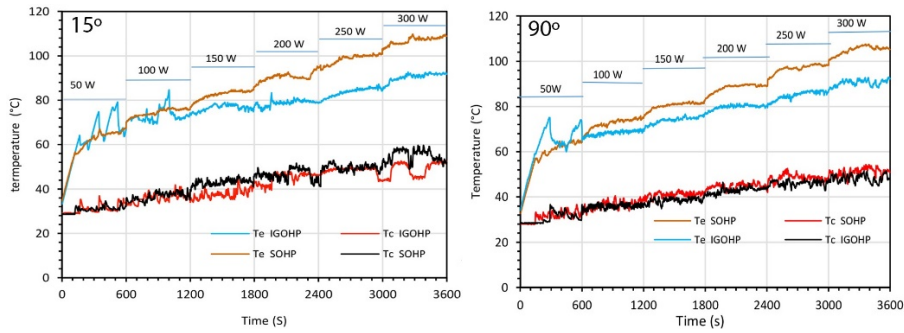


Fig.9. Comparison of transient evaporator and condenser temperatures for IGPHP and SPHP system, inclination angle 15° left and 90° right

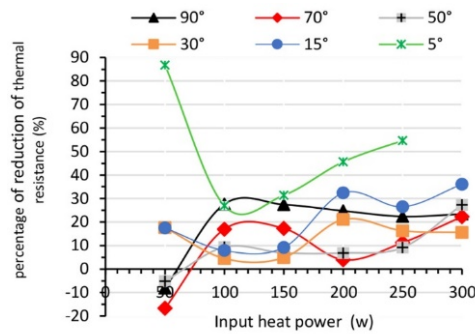


Fig. 10. Percentage of thermal resistance reduction for IGPHP in comparison to SPHP, different angles and input heat

Fig. 10 shows the percentage decrease of the thermal resistance for IGPHP relative to SPHP system (negative values showing that thermal resistance has increased). In general, the thermal resistance of IGPHP compared to SPHP has decreased in all angles (except at 50W and angles of 50°, 70°, and 90°). The average value of decrease is about 21% across all angles and input heat values. However, the highest decrease is shown at a low inclination angle of 5° with a 49% reduction. Considering that prior research has illustrated a poor performance for the SPHP at small angles, the results of Fig. 10 shows that performance of the PHPs can be improved at low angles (except below 5°) by using IGPHP system.

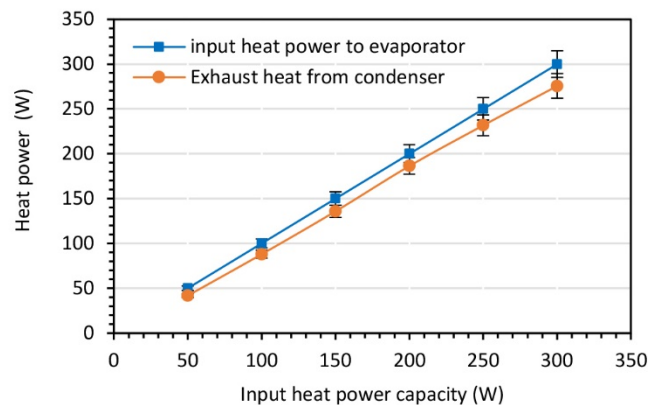


Fig. 11. Comparison of rate of heat input into the evaporator and output from condenser

Fig. 11 illustrates energy balance by comparing the rate of thermal energy input to the evaporator and lost through condenser in different heat inputs. The values obtained using average temperature difference of working fluid inlet and outlet and flow rate values. The results show less than 10% heat loss in the system that is expected due to the losses through insulation surface and the PHP body.

## 4. Conclusions

In this experimental study, the thermal performance of Inner-Grooved Pulsating Heat Pipes (IGPHP) and Smooth Pulsating Heat Pipes (SPHP) compared using distilled water as working fluid in different angles and different input heat powers. The range of inclination angles of 0°, 5°, 15°, 30°, 50°, 70°, and 90°, and the Input heat powers of 50W, 100W, 150W, 200W, 250W, and 300W were studied. The comparison of thermal power input to the evaporator and output from the condenser is showing on average less than 10% reduction in the energy output; that is the heat loss through insulation and other surfaces in the system. The following conclusions were obtained:

1. The filling ratio of 60% was found an optimum value for both IGPHP and SPHP systems, therefore this value was used for all experiments in this research. The results show that start-up pulsation occurs later in IGPHP compared to the SPHP across all ranges in this study. However, the start-up pulsation of IGPHP occurs closer to SPHP in lower inclination angles.
2. The IGPHP system at an inclination angle of 0° showed high thermal resistance leading to dryout phenomenon at input heat power of 100W. However, for SPHP, the dryout took place at an angle of 5° and input heat power of 250W.
3. The results show that condenser temperature for both IGPHP and SPHP remains relatively equal in the range of inclination angles and input heat powers used in this research. However, the evaporator temperature (except for input heat of 50W) is higher in SPHP compared to the IGPHP system. Therefore, the evaporator temperature difference and consequently, thermal resistance are lower for IGPHP relative to the SPHP systems, while the effective thermal conductivity value is higher for IGPHP.
4. The average reduction of thermal resistance in IGPHP across all angles and input heat values was found 21% relative to SPHP. The IGPHP leads to improved thermal performance across all experiments in this study except at 50W at angles of 50°, 70°, and 90°. An average thermal resistance reduction of 49% occurred for IGPHP compared to the SPHP at an inclination angle of 5° across all the heat capacities in this study. Therefore, IGPHP could be an excellent alternative to SPHP in low inclination angles, where SPHP performs poorly.
5. The results show that the thermal performance of IGPHP is consistently higher compared to the SPHP across all angles for input heat powers of 250W and 300W, suggesting that IGPHP could be performing even better in higher PHP capacities.

## References

- [1] Akachi H., Structure of a heat pipe. USA, Patent 4921041, 1990.
- [2] H. Ma, Oscillating heat pipes. Springer, (2015).
- [3] Y.H. Lin, S.W. Kang, and H.L. Chen, Effect of silver nano-fluid on pulsating heat pipe thermal performance, Applied Thermal Engineering, 82 (11) (2008) 1312-1317
- [4] F. Mobadersani, S. Jafarmadar, A. Rezavandc, Modeling of A Single Turn Pulsating Heat Pipe based on Flow Boiling and Condensation Phenomena. International Journal of Engineering, 32, (4) (2019) 569-579.
- [5] C. Jung, S. J. Kim, Effects of oscillation amplitudes on heat transfer mechanisms of pulsating heat pipes ,International Journal of Heat and Mass Transfer, 165 (2021) 120642
- [6] X. Suna, . Lia, B. Jiao, Z. Gan, J. Pfothenauerd, B. Wang, Q. Zhao, D. Liue, Experimental study on hydrogen pulsating heat pipes under different number of turns, cryogenics, 111 (2020) 103174
- [7] Yang H., Wang J., Wang N., Yang F., Experimental study on a pulsating heat pipe heat exchanger for energy saving in air-conditioning system in summer. Energy and Buildings. Volume 197, 15 August, 1-6, 2019.
- [8] M. Winkler , D. Rapp, A. Mahlke, F. Zunftmeister, M. Vergez,E. Wischerho, J. Clade, K. Bartholomé , O. S.-Welsen ,Small-Sized Pulsating Heat Pipes/Oscillating Heat Pipes with Low Thermal Resistance and High Heat Transport Capability, Energies, 13 (7) (2020) 1736

- [9] R. Borkar, P. Pachghare, Thermo-Hydrodynamic Behavior of Methanol Charged Closed Loop Pulsating Heat Pipe. *Frontiers in Heat Pipes (FHP)*, 5 (1) (2014) 01-07.
- [10] B. Markal, R. Varo, Experimental investigation and force analysis of flat-plate type pulsating heat pipes having ternary mixtures, *International Communications in Heat and Mass Transfer*, 121 (2021) 105084
- [11] J. Qu, X. Li, Q. Xu, and Q. Wang, Thermal performance comparison of oscillating heat pipes with and without helical micro-grooves, *Heat and Mass Transfer* 53 (2017) 3383–3390.
- [12] A. I. Nowak, C. Czajkowski, P. Błasiak, S. Pietrowicz, Thermal Performances Of A Pulsating Heat Pipe With Different Inclination Angles, Filling Ratios and Working Fluids. *International Symposium on Oscillating/Pulsating Heat Pipes*, Daejeon, Korea, 25-28 September (2019).
- [13] S. A. Jahan, M. Ali, M.Q. Islam, Effect of inclination angles on heat transfer characteristics of a closed loop pulsating heat pipe (CLPHP). *Procedia Engineering* 56 (2013) 82 – 87.
- [14] S. B. Paudel, G. J. Michna, effect of inclination angle on pulsating heat pipe performance. *Proceedings of the ASME 12th International Conference on Nanochannels, Microchannels, and Minichannels*. August 3-7, Chicago, Illinois, USA, (2014).
- [15] H. R. Goshayeshi, M. Goodarzi, M. R Safaei, M. Dahari, Experimental Study on the Effect of Inclination Angle on Heat Transfer Enhancement of a Ferrofluid in a Closed Loop Oscillating Heat Pipe under Magnetic Field. *Experimental Thermal and Fluid Science*, 74 (2016) 265–270.
- [16] M. Li, L. Li, D. Xu, Effect of filling ratio and orientation on the performance of a multiple turns helium pulsating heat pipe. *Cryogenics*. Volume 100 (2019) 62-68.
- [17] J. Lee, Y. Joo, S. J. Kim, Effects of the number of turns and the inclination angle on the operating limit of micro pulsating heat pipes, *International Journal of Heat and Mass Transfer*, (124) (2018) , 1172-1180
- [18] L. A. Betancur, M. J. P. Flórez, M. H. Mantelli, Experimental study of channel roughness effect in diffusion bonded pulsating heat pipes, *Applied Thermal Engineering*, 166 (2020) 114734
- [19] S. J. Kim, J. K. Seo, K. H. Do, Analytical and experimental investigation on the operational characteristics and the thermal optimization of a miniature heat pipe with a grooved wick structure. *International Journal of Heat and Mass Transfer*, 46 (2003) 2051–2063.
- [20] D. Xu , T. Chen , Y. Xuan, Thermo-hydrodynamics analysis of vapor–liquid two-phase flow in the flat-plate pulsating heat pipe, *International Communications in Heat and Mass Transfer*, 39 (4) ( 2012) 504-508
- [21] T. Hao, X. H. Ma, Z. Lan, N. Li, Y.Z. Zhao, H.B. Ma, Effects of hydrophilic surface on heat transfer performance and oscillating motion for an oscillating heat pipe. *Int. J. Heat and Mass Transfer*, 72 (2014) 50–65.
- [22] T. Hao, X. Ma, Z. Lan, N. Li, Y. Zhao, Effects of superhydrophobic and superhydrophilic surfaces on heat transfer and oscillating motion of an oscillating heat pipe. *J. Heat Transfer*, 136 (2014) 082001-13.
- [23] Y. Ji, C. Xu, H.B. Ma, X. Pan, An experimental investigation of the heat transfer performance of an oscillating heat pipe with copper oxide (CuO) microstructure layer on the inner surface. *J. Heat Transfer*, 135 (2013) 074504-4.
- [24] J.J. Xu, Y.W. Zhang, H.B. Ma, Effect of internal wick structure on liquid-vapor oscillatory flow and heat transfer in an oscillating heat pipe. *J. Heat Transfer* 131 (2009) 121012-10.
- [25] A.J. Jiao, R. Riegler, Ma H.B., Peterson G.P., Thin film evaporation effect on heat transport capability in a grooved heat pipe. *Microfluid Nanofluid*, 1 (2005) 227–233.
- [26] L.L. Vasiliev, Micro and miniature heat pipes – electronic component coolers. *Applied Therm Eng.*, 28 (2008) 266–273.
- [27] A. Faghri, Review and advances in heat pipe science and technology. *J. Heat Transfer*, 134 (2012) 123001-18.
- [28] F.Z. Zhang, R.A. Winholtz, W.J. Black, M.R. Wilson, H. Taub, H.B. Ma, Effect of hydrophilic nanostructured cupric oxide (CuO) surfaces on the heat transport capability of a flat plate oscillating heat pipe. *J. Heat Transfer*, 138 (2016) 062901-7.
- [29] J. Qu, X. Li, Q. Xu, Q. Wang, Thermal performance comparison of oscillating heat pipes with and without helical micro-grooves. *Heat and Mass Transfer*, 53 (2017) 3383–3390.
- [30] M.A. Kedzierski, J.M. Goncalves, Horizontal convective condensation of alternative refrigerants within a micro-fin tube, *Journal of Enhanced Heat Transfer* 6 (2) (1999) 161–178.
- [31] S. Khandekar, Thermo-hydrodynamics of closed loop pulsating heat pipes, *Doctoral Engineer (Dr.-Ing.) thesis*, University of Stuttgart, Stuttgart, Germany, 2004.
- [32] C. Sun, C. Tseng, K. Yang, S. Wu, C. Wanga, Investigation of the evacuation pressure on the performance of pulsating heat pipe, *International Communications in Heat and Mass Transfer*, 85 (2017) 23-28.
- [33] J. Qu, Q. Wang, Experimental study on the thermal performance of vertical closed-loop oscillating heat pipes and correlation modeling. *Applied Energy*, 112 (2013) 1154–1160.
- [34] C. M. Douglas, *Design and analysis of experiments*, John Wiley and sons. 2001